Effect of Ferrite Transformation on the Tensile and Stress Corrosion Properties of Type 316 L Stainless Steel Weld Metal Thermally Aged at 873 K

H. SHAIKH, H.S. KHATAK, S.K. SESHADRI, J.B. GNANAMOORTHY, and P. RODRIGUEZ

This article deals with the effect of the microstructural changes, due to transformation of delta ferrite, on the associated variations that take place in the tensile and stress corrosion properties of type 316 L stainless steel weld deposits when subjected to postweld heat treatment at 873 K for prolonged periods (up to 2000 hours). On aging for short durations (up to 20 hours), carbide/carbonitride was the dominant transformation product, whereas sigma phase was dominant at longer aging times. The changes in the tensile and stress corrosion behavior of the aged weld metal have been attributed to the two competitive processes of matrix softening and hardening. Yield strength (YS) was found to depend predominantly on matrix softening only, while significant changes in the ultimate tensile strength (UTS) and the work-hardening exponent, n, occurred due to matrix hardening. Ductility and stress corrosion properties were considerably affected by both factors. Fractographic observations on the weld metal tested for stress-corrosion cracking (SCC) indicated a combination of transgranular cracking of the austenite and interface cracking.

I. INTRODUCTION

THE use of austenitic stainless steels as prime construction materials for liquid metal-cooled fast breeder reactors often necessitates the joining of two or more components by the process of welding. High-temperature delta ferrite is deliberately retained in the weld metal to overcome the problem of hot cracking during weld metal solidification.[1] The use of these welded components at elevated temperature would result in the time-dependent degradation of the material, particularly of the weld metal, because the delta ferrite component of the duplex weld metal transforms to carbides/carbonitrides and intermetallic phases, such as the sigma phase, small quantities of which lead to large variations in the tensile[2,3] and corrosion properties.[4–7]

No two investigators have reported matching results for the transformation kinetics of delta ferrite[3,8] because of a large number of variables in a weld, such as chemical composition of the weld metal, size and shape of the delta ferrite, diffusion of chromium in the ferrite, service temperature, *etc*. The kinetics of the ferrite transformation as well as the type and amount of the precipitated phases mainly depend on the carbon content and the concentration of elements that promote sigma formation in the weld metal.[9,10] The tendency toward sigma phase formation can be quantitatively determined using Hull's equation, by which the steel would be susceptible to sigma phase embrittlement if the "equivalent chromium number" (ECN) exceeds approximately 17.8 wt pct.[11] The transformation kinetics of the delta ferrite and the nucleation and growth of the sigma phase[12] are faster when stainless steels contain low concentrations of carbon. The size and shape of the delta ferrite[10] also govern the transformation kinetics of the weld metal. Kokawa *et al.*[13] have reported that at 973 K, sigma precipitation occurs much earlier in the vermicular ferrite than in the lacy ferrite.

Microstructurally, low-temperature aging (<973 K) reduces ferrite to secondary austenite and carbides/carbonitrides,[3,9,14,15] and therefore, the precipitation of sigma phase is retarded. However, at high temperatures (>973 K), the ferrite dendrites transform directly to sigma and very few carbides/carbonitrides are obtained, although precipitation of chi and austenite phases has been observed.[12,16]

Tensile studies of duplex weld metal indicated that at room temperature, delta ferrite strengthens the weld metal, in comparison with the base metal, as evidenced by increases in the yield strength (YS) and ultimate tensile strength (UTS) accompanied by reduction in elongation.[17] The competitive processes of annealing and transformation of ferrite govern the changes in the tensile properties during high-temperature aging of the weld metal.[2]

Studies on stress-corrosion cracking (SCC) behavior of the duplex weld metal of austenitic stainless steels showed that its SCC resistance depends on the content, distribution, and solidification mode of the ferrite.[18,19] A duplex weld metal could fail by a combination of SCC of austenite and either (1) delta ferrite-austenite interface cracking[20,21] or (2) stress assisted dissolution of ferrite.[18,22] A fully austenitic weld could fail by intergranular stress-corrosion cracking (IGSCC).[19] A continuous network of delta ferrite was found to be most

H. SHAIKH and H.S. KHATAK are Scientific Officers, J.B. GNANAMOORTHY is the Head of the Metallurgy Division, and P. RODRIGUEZ is Director, Indira Gandhi Centre for Atomic Research, Kalpakkam, India. S.K. SESHADRI, Associate Professor, is with the Department of Metallurgical Engineering, Indian Institute of Technology, Madras, India.

Manuscript submitted April 16, 1992.

harmful. Although the SCC behavior of duplex weld metal has been investigated, no significant studies have been reported on the effect of high-temperature aging on its SCC susceptibility. The effects of annealing and precipitation of various intermetallic phases, besides the chromium depletion of the matrix, are expected to considerably affect the SCC susceptibility of the weld metal. The present study correlates the microstructural changes, that occur in type 316 L stainless steel weld deposits on aging at 873 K for prolonged periods (up to 2000 hours), to the observed variations in the tensile and stress corrosion behavior.

II. EXPERIMENTAL PROCEDURE

Bead-on-plate weld deposits (Figure 1) were prepared from AISI type 316 L stainless steel filler wire (chemical composition in Table I) using the gas tungsten arc welding (GTAW) process (welding parameters in Table II). The weld deposits were susceptible to sigma phase formation since the ECN was 20.63. The effect of dilution was eliminated by machining off 10 mm of the deposit from the base plate. Flat tensile specimens (Figure 2) were made along the length from defect-free undiluted weld deposits. The samples were subsequently aged in a tubular furnace at 873 K for time periods of 2, 20, 200, and 2000 hours.

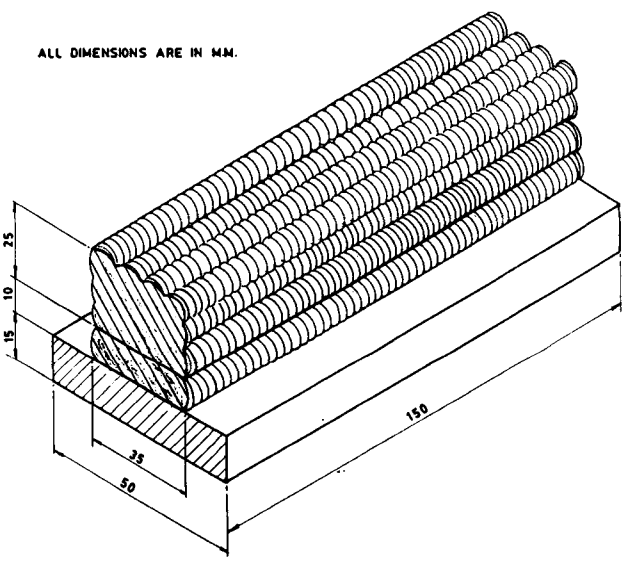

Fig. 1—A schematic of the bead-on-plate weld pad.

Table I. Chemical Composition (in weight percent) of AISI Type 316 L Stainless Steel Filler Wire and its Weld Deposit

Element	Filler Wire	Weld Deposit
Ni	11.4	10.8
Cr	18.7	18.7
Mo	2.34	2.10
C	0.024	0.022
Mn	—	1.74
Si	0.38	0.36
S	0.002	0.002
P	0.02	0.02
N	—	0.026

The delta ferrite content of the weld metal was measured before and after aging using a magne-gage. The total amount of secondary phases present in the aged weld metals was estimated by electrochemical extraction technique which was carried out in a methanol solution containing 10 pct (by volume) HCl, at a potential of 1.5 V with respect to the platinum electrode.[23] The residue obtained by the electrochemical extraction process was identified by the X-ray diffraction technique. Optical microscopic examinations of the as-deposited and aged weld metals were carried out. The as-deposited weld metal and the weld metal aged for 2 hours were chemically etched with Murakami reagent (10 g potassium ferricyanide and 10 g potassium hydroxide in 100 mL water) for 3 minutes. The other thermally aged samples were etched in a modified Murakami reagent (20 g potassium ferricyanide and 20 g potassium hydroxide in 100 mL of water) for about 15 seconds at 363 to 368 K.

Stress-corrosion studies were carried out using the constant extension rate testing (CERT) technique and the constant load (CL) technique. In the CERT technique, the tests were carried out at a nominal strain rate of 5.5×10^{-5} /s in 45 pct magnesium chloride solution at 427 K. Constant load tests were conducted in 45 pct magnesium chloride solution at 427 K at an initial stress level of 40 pct yield stress.

Tensile properties were evaluated in liquid paraffin at a temperature of 427 K and a nominal strain rate of 5.55×10^{-5}/s. Microhardness measurements of the austenite matrix were also carried out.

The fracture surfaces of the samples tested for SCC using both the CERT and constant load techniques were

Table II. Gas Tungsten Arc Welding Parameters

Welding process	GTAW (manual)
Welding wire	AWS-ER 316L
Shielding gas	Ar
Polarity	DC electrode negative
Welding voltage	20 volts
Welding current	100–110 A
Welding speed*	1.0×10^{-3} m/s
Wire feed rate*	1.5×10^{-3} m/s
Ar flow rate	75×10^{-6} m^3/s

*The wire feed rate and the welding speed represent approximate average values because the welding was carried out manually.

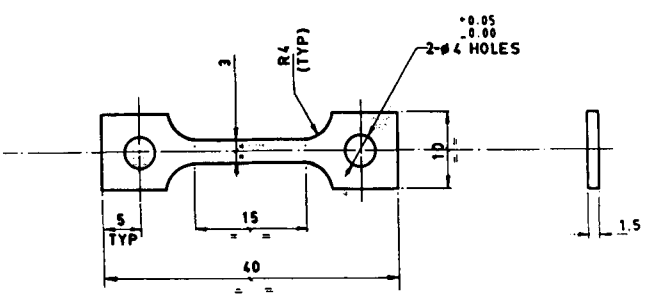

Fig. 2—A schematic of the flat tensile samples used in the study.

examined in a scanning electron microscope (SEM) to study the cracking mode.

III. RESULTS AND DISCUSSION

A. *Transformation Kinetics of Delta Ferrite*

The average ferrite content of the as-deposited weld metal was determined to be 7 FN (ranging from 5.4 to 9.1 FN) with a standard deviation of ±0.7 FN. The ferrite content before and after aging at 873 K was converted to the fraction of the delta ferrite transformed and plotted in Figure 3 as a function of aging time. The figure indicates a decrease in the transformation rate with increasing aging time.

Figure 4, which depicts the variation in the total amount of precipitates extracted with aging time up to 2000 hours, indicates a continuous increase in the amount of second phases precipitated. As in Figure 3, a decrease in the precipitation rate is observed with increasing aging time.

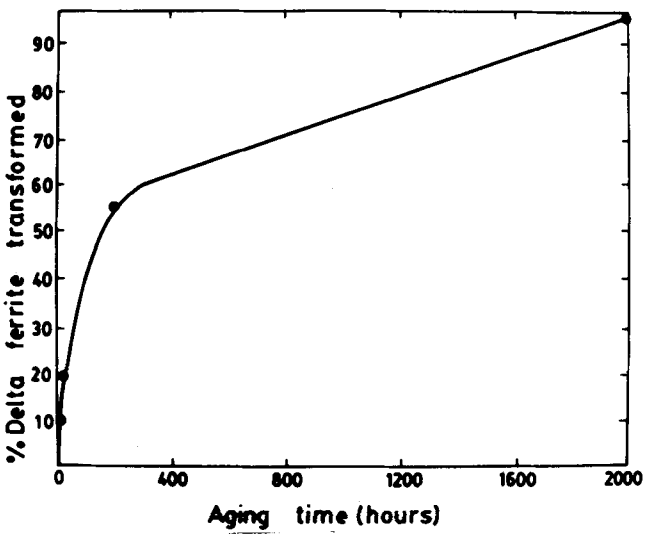

Fig. 3—Transformation kinetics of delta-ferrite.

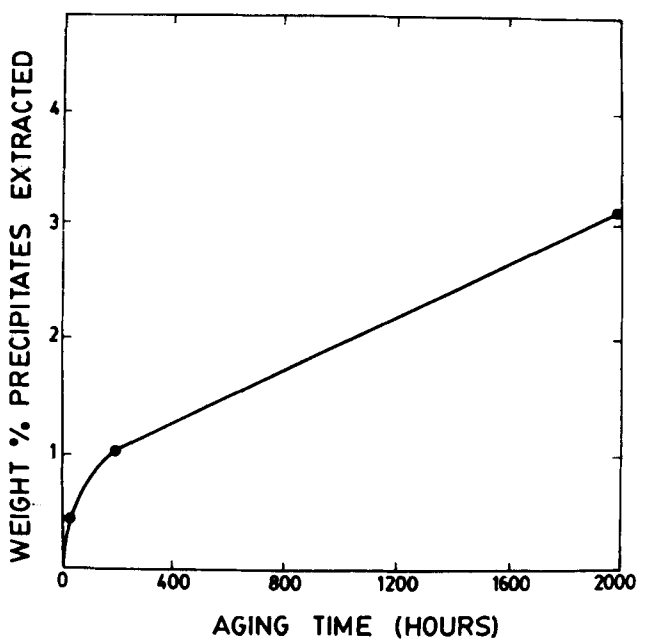

Fig. 4—Dependence of amount of precipitates extracted on aging time at 873 K.

The various phases present in the electrochemical residue (Table III) were identified in accordance with the Standard ASTM X-ray diffraction practices. The dominant phase on aging at 2 hours was delta ferrite, whereas on 20 hours of aging, carbides/carbonitrides were found to be the significant phase. Aging of the weld metal for 20 hours did not indicate sigma phase in the X-ray diffraction (XRD) pattern. Sigma phase was the dominant phase on aging up to 200 and 2000 hours. The amount of sigma phase present was greater in the latter case. Another intermetallic phase, whose index values correspond to the *R* phase, was found in increasing quantities up to 200 hours of aging. Its presence was not detected on aging to 2000 hours. Lai and Haigh,[15] Thomas and Keown,[9,24] and Tavassoli *et al.*[25] reported the presence of *R* phase in austenitic stainless steel weld metal. This phase has a hexagonally close-packed structure[15,25] and precipitates inside the ferrite with a lathy morphology.[9,14,25] Formation of *R* phase has been reported during stress relief of austenitic weldments containing higher amounts of ferritizers in the weld metal.[9] Tavassoli *et al.*[25] reported its presence on aging of Mo bearing alloys.

Based on the dominance of carbides/carbonitrides in the electrochemical residues of weld metal aged up to 20 hours, it was inferred that up to this aging time, the ferrite transformed by the reaction

$$\text{delta ferrite} \rightarrow \text{carbide/carbonitride} + R \text{ phase} \quad [1]$$

Lai and Haigh[15] reported that at lower aging temperatures, delta ferrite transformed mainly to austenite and carbides/carbonitrides which precipitated within the delta ferrite as well as at the delta ferrite-austenite interface. Slattery *et al.*[12] reported a similar reaction on aging at 898 K. Leitnaker *et al.*[26] stated that the precipitation of carbides/carbonitrides enriched in Cr and in Mo depleted the ferrite of these elements. This depleted ferrite was then either retained or transformed to austenite.

The preponderance of the sigma phase in the electrochemical residues of samples aged up to 200 and

Table III. Results of the X-Ray Diffraction Studies Showing the Abundance of Various Phases in the Weld Metal Aged for Various Durations of Time

Aging time (h)	Phases Identified (with Relative Abundance)
2	$\delta > C$
20	$C > R$
200	$\sigma > C > R$
2000	$\sigma > C$

δ is delta ferrite
C is carbide/carbonitride
R is R phase
σ is sigma phase

2000 hours indicated that on aging for these durations of time, the following transformation reaction occurred

$$\text{delta ferrite} \rightarrow \text{sigma} + \text{carbide/carbonitride} \quad [2]$$

The presence of carbide/carbonitride phase in the electrochemical residues of samples aged for 200 and 2000 hours suggested that the delta ferrite to carbide/carbonitride reaction occurred in the early stages of aging. Sigma phase precipitation in the retained depleted ferrite was then facilitated by the diffusion of sigma phase formers, like Cr and Mo, from austenite to delta ferrite. The decrease in the transformation rate of ferrite and precipitation rate of second phases (Figures 3 and 4) could be explained based on (1) the time taken for reduction of carbon content in the ferrite, to values at which sigma phase precipitation is facilitated; and on (2) the time taken for critical amounts of sigma forming elements to diffuse from austenite matrix to the depleted ferrite.

Optical micrographs in Figure 5(a) through (e) are for as-deposited weld metal and for weld metal aged for 20, 200, and 2000 hours, respectively. Figure 5(a) indicates discontinuous and predominantly lacy ferrite morphology in the as-deposited weld metal, although vermicular morphology is also observed at some areas. The predominance of fine lacy ferrite could be due to the high cooling rates involved in the bead-on-plate weld deposits. Figure 5(b) shows the transformed second phases as small dark dots in the ferrite particles of the weld metal aged for 20 hours. Micrographs in Figures 5(c) through

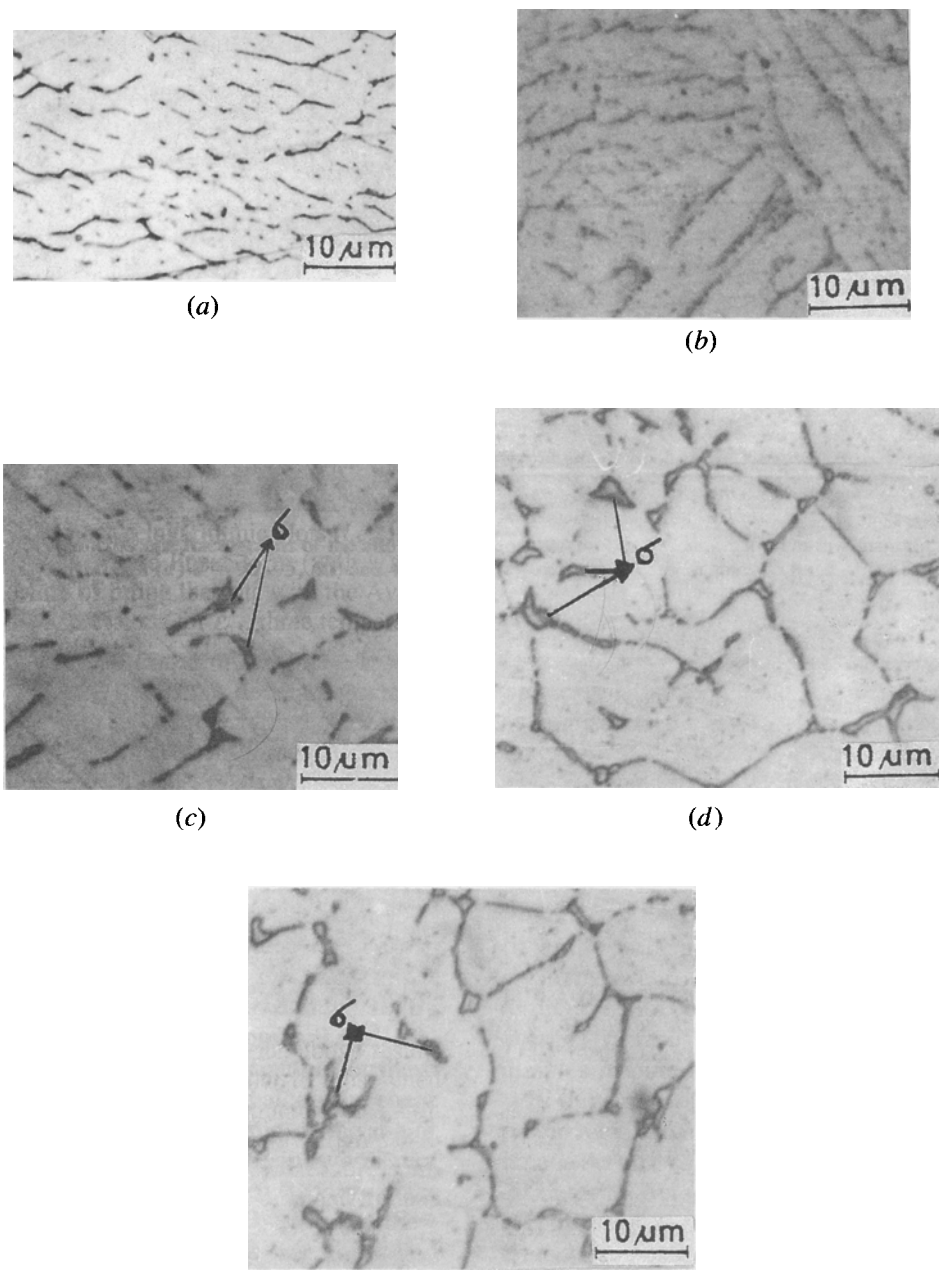

Fig. 5—Optical micrographs of weld metal aged at 873 K for (*a*) 0 h, (*b*) 20 h, (*c*) and (*d*) 200 h, and (*e*) 2000 h.

(e) of the samples aged for 200 and 2000 hours show large, elongated sigma phase particles in the microstructure both in the form of a continuous network and as separate particles. The presence of both lacy and vermicular delta ferrite in the weld metal caused such variations in the microstructure on high-temperature aging because of the differences in the coherency of their interfaces with austenite. Kokawa *et al.*[13] stated that the lower the delta/gamma boundary coherency, the easier the sigma precipitation. Since this coherency was high in the lacy ferrite and lower in the vermicular type, sigma precipitation started early in the vermicular ferrite.[13] Heat treatments for long durations would result in the sigma precipitation reaction taking place in the lacy ferrite too. Hence, the ferrite particles in which the sigma precipitates appear as dark dots in Figure 5(c) and as near-continuous sigma networks in one region of Figure 5(d) and (e) could be the regions of lacy ferrite. Regions showing near-continuous network of sigma in Figure 5(c) and separate sigma particles in Figures 5(d) and (e) could be the regions of vermicular ferrite.

B. *Effect of Aging on the Tensile Properties of the Weld Metal*

This section relates the changes in tensile properties of the weld metal to (1) microstructural evolution accompanying delta ferrite transformation, (2) amount of second phases precipitated, and (3) consequent effect of these on the austenite matrix. The temperature and the strain rate selected were the same as those used in the CERT technique for SCC. A plot indicating the change in YS with aging time is shown in Figure 6. The YS continuously decreased up to 200 hours of aging, after which the trend was slightly reversed on aging up to 2000 hours. The drop in YS was significant on aging the weld metal for 2 hours. This drop in YS on aging could be attributed to one, or more, of the following reasons: (1) depletion of the solid solution strengtheners like Cr, Mo, C, and N in the austenite due to the nucleation and growth of sigma and carbide phases; (2) dissolution of delta ferrite; and (3) decrease in the dislocation density in the austenite on aging.[9] Thomas and Yapp reported that the decrease in the YS was a result of thermal recovery,[3] but Gill *et al.*[2] attributed the drop in YS to depletion of solid solution strengtheners and dissolution of ferrite, since no evidence of cell formation and decrease in the dislocation density was available on aging the weld metal for 5000 hours at 873 K.

Figure 7 shows that the UTS increases slightly on aging up to 200 hours and significantly on aging up to 2000 hours. The slight increase in the UTS on aging up to 200 hours could be due to the formation of a thin film of carbide/carbonitride at the austenite/delta ferrite interface and the absence of considerable amounts of sigma phase in the microstructure. The significant increase in the UTS on aging up to 2000 hours was due to the presence of a large amount of sigma phase in the microstructure. The amount, size, shape, and distribution of the phases that precipitate from delta ferrite are reported to significantly affect the UTS.[2,3]

Figure 8 indicates a continuous, although slight, increase in ductility on aging up to 200 hours, after which a decrease is observed on aging to 2000 hours. The increase in the ductility could be attributed to the factors

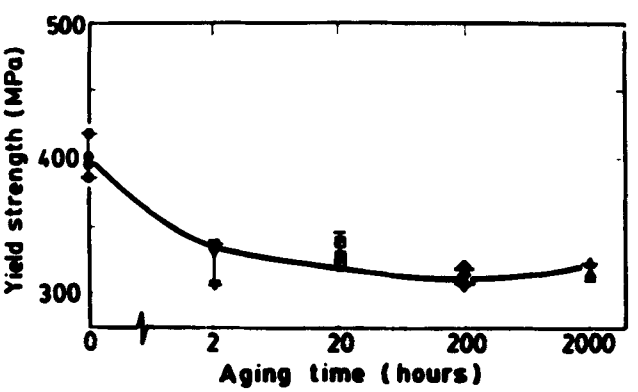

Fig. 6—Effect of aging time at 873 K on yield strength.

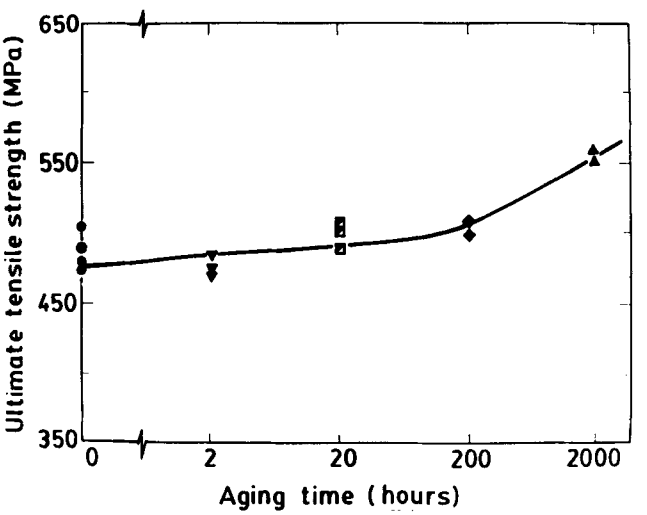

Fig. 7—Dependence of UTS on aging time at 873 K.

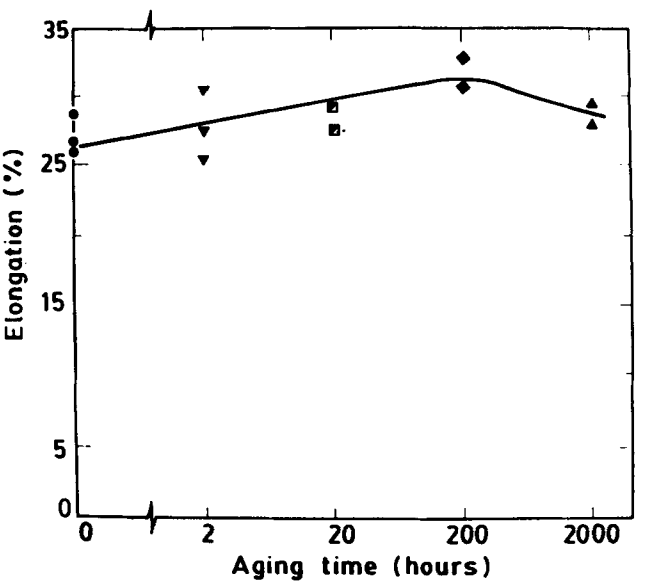

Fig. 8—Variation in ductility as a function of aging time at 873 K.

that cause a decrease in the YS. The decreased ductility on aging up to 2000 hours, as compared to that after 200 hours of aging, may be due to the presence of significant amounts of sigma phase in the microstructure. Although Thomas and Yapp[3] reported similar results, Gill *et al.*[2] reported a marked decrease in the ductility through all aging times at all aging temperatures.

The work-hardening exponent, n, was numerically, evaluated using a nonlinear curve fitting program, VB01A, of Harwell Library. Figure 9 shows that the value of n increases gradually on aging up to 200 hours and substantially on aging up to 2000 hours. The small increase in the value of n on aging up to 200 hours may be due to the insignificant increase in the total amount of precipitates in the matrix. The significant increase in the value of n on aging up to 2000 hours resulted from the considerable increase in the total amount of precipitates, which were comprised mainly of the nondeformable sigma phase. The increase in the total quantity of precipitates led to increased particle-dislocation interaction and thus an increase in the value of n.

Figure 10 shows that the microhardness of the austenite matrix gradually decreased on aging up to 200 hours, after which an increase in the matrix hardness was observed on aging up to 2000 hours. The microhardness results give conclusive evidence of the inference that the high-temperature tensile properties of a type 316 L weld metal depend on the following two competing factors:

(1) softening of the matrix as a result of loss of solid solution strengtheners and dissolution of delta ferrite (this would have an effect on the YS, microhardness, and ductility); and

(2) hardening of the matrix by the precipitation of significant amounts of nondeformable sigma phase (this affected all the properties other than YS).

C. *Effect of Aging on the Stress-Corrosion Properties of the Weld Metal*

The discussions in Section B suggest that the time-dependent changes in the tensile properties of the weld metal on aging at 873 K depend on the two competitive processes of matrix softening and hardening. Apart from the preceding two processes, the depletion of Cr and Mo from the austenite matrix would also affect corrosion resistance of weld metal on high-temperature aging.

The CERT technique results in liquid paraffin and in $MgCl_2$, at 427 K, were compared to evaluate the SCC resistance based on the ratios of values of UTS and percent elongation in the two tests, along with the SCC susceptibility index, I, which is defined as l ratio of values of UTS $\times$ percent elongation in the two tests.[27] Figure 11 shows a deterioration in the SCC resistance on aging to 2 hours with little change thereafter on further aging.

The observations in Figure 11 were verified by calculating average crack propagation rates (CPR) using the formulas proposed by Desestret and Oltra[28] and by Hishida *et al.*[29] The formula proposed by Desestret and Oltra bases the calculation of the CPR on the ratios of values of fracture stresses in $MgCl_2$ and in liquid paraffin. Hishida *et al.*[29] suggested the use of the value of the work-hardening exponent to calculate the average CPR. Since flat tensile samples were used for the current study and since the cracking initiated at all four corners, the calculations of the CPR were based on the initial area of the specimen and not on the initial radius of the specimen as suggested in Eqs. [1] and [2]. The time-to-failure, t_f (Table IV), used to calculate the CPR was considered as the time spent by the weld metal between the YS and the maximum load in $MgCl_2$. The YS was used as the initial criteria to calculate t_f, because little difference was observed in the values of YS in the tests carried out both in liquid paraffin and in $MgCl_2$. Beyond the maximum load, the material fails by pure ductile failure. Figure 12 shows an improvement in the SCC resistance up to 200 hours of aging (decreasing CPR) and a deterioration at 2000 hours of aging. The CPR values obtained using Hishida's formula were nearly one-third of those obtained by using Desestret and

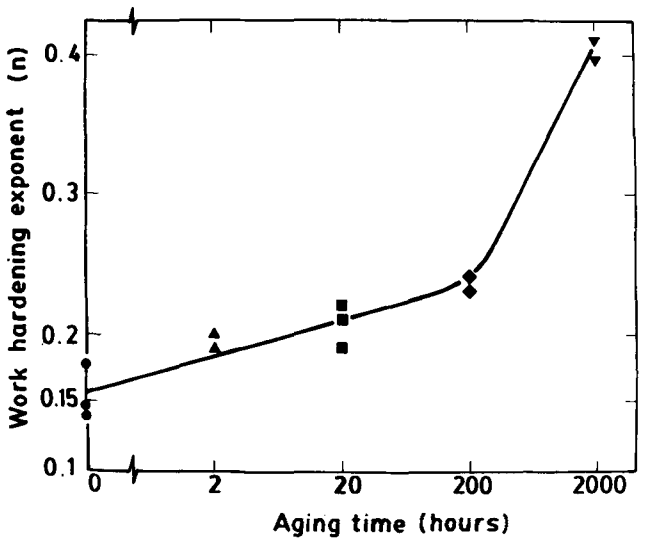

Fig. 9—Rate of change in work-hardening exponent with aging time at 873 K.

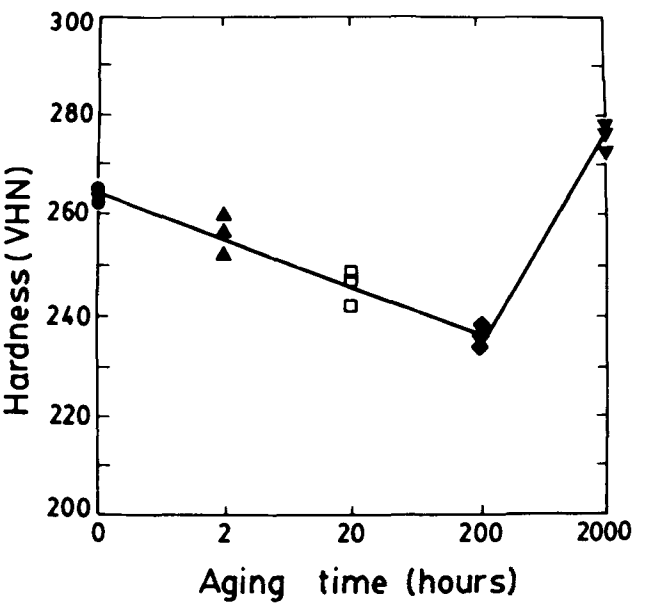

Fig. 10—Variation in the microhardness of the austenite matrix with aging time at an aging temperature of 873 K.

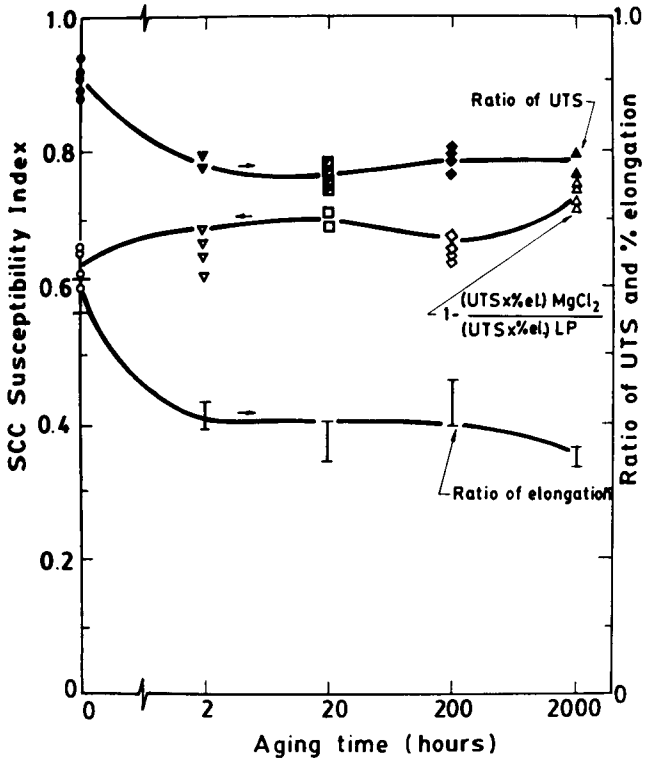

Fig. 11—Variation in the SCC susceptibility as a function of aging time at an aging temperature of 873 K.

Table IV. The Average Residence Time in the Region Between YS and Maximum Load in Boiling 45 Percent $MgCl_2$ (427 K) for the Weld Metals of Various Heat-Treatment Durations

Aging Time (h)	Average Residence Time (min)
0	6
2	6.9
20	10.4
200	15
2000	12

Oltra's formula. These results are contrary in trend to those obtained by using the assessment parameters in Figure 11, thus indicating that the evaluation parameters are of paramount importance in assessing the results of the CERT experiments.

A careful choice of the evaluation parameters is necessary when assessing materials with differing tensile properties, using the CERT tests, as in the present case. The conventionally used parameters like the ratios of values of UTS and percent elongation in $MgCl_2$ and liquid paraffin along with the cracking index could give error-prone conclusions in such cases. Similar opinions have been expressed by Kim and Wilde[30] and Khatak *et al.*,[31] both of whom expressed skepticism on the use of the CERT technique for comparing the susceptibility of alloys with widely differing microstructures, ductility, and strength levels. Khatak *et al.* suggested the use of the average CPR calculated by the Desestret and Oltra formula.[32]

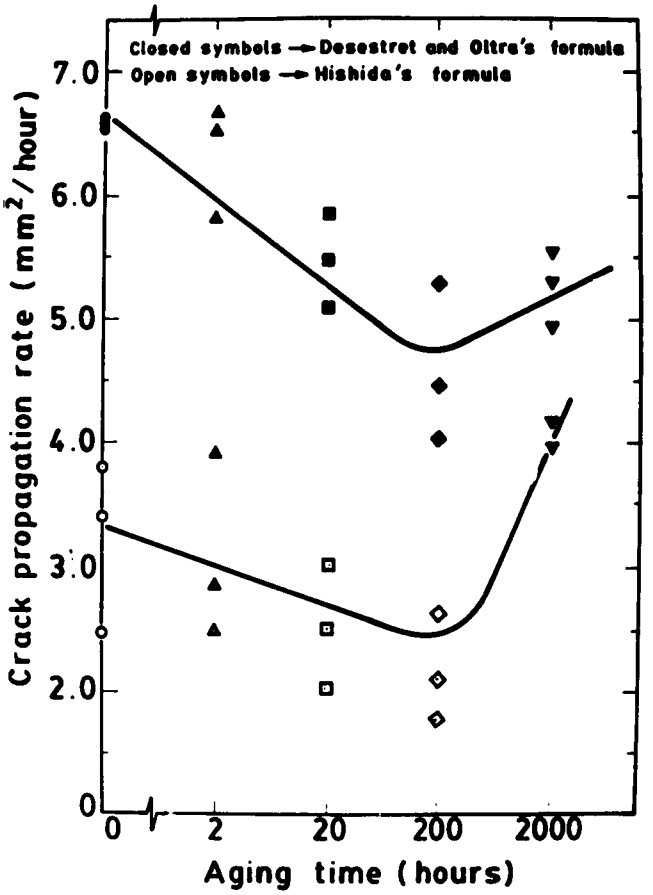

Fig. 12—Dependence of crack propagation rates on aging time at 873 K.

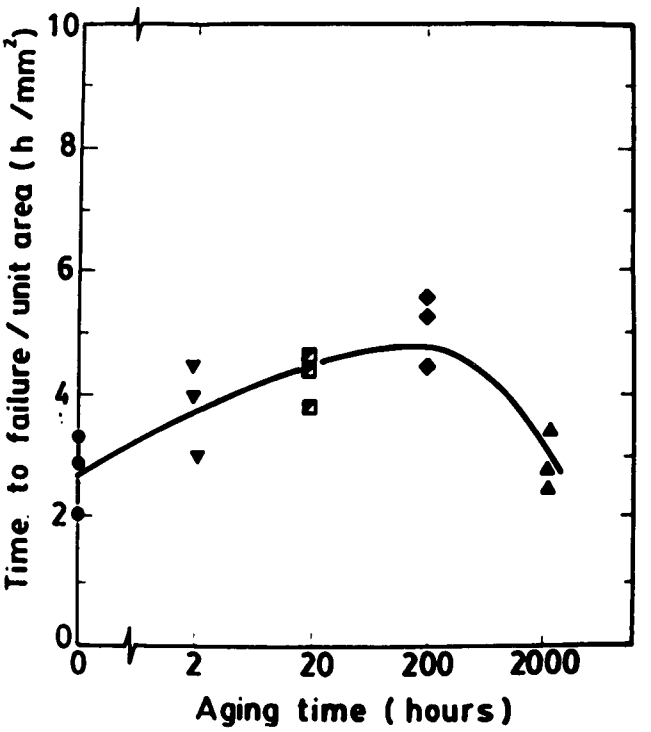

Fig. 13—Dependence of time-to-failure (in constant load tests) on aging time at an aging temperature of 873 K.

The contradiction in the assessment of the CERT data was resolved by testing for SCC using the constant load technique at 40 pct of YS. These tests indicate that the t_f per unit area of the test specimen increases with increasing aging time up to 200 hours of aging and decreases thereafter on aging to 2000 hours (Figure 13). Since the constant load tests were carried out using a fraction of the YS of the material, the results obtained were considered reliable.[32] The trend observed in Figure 12 is in agreement with the results obtained in the constant load tests.

The increased SCC resistance for the weld metal aged between 0 and 200 hours is related to the decrease in YS with increasing aging time. The increase in the SCC resistance could be explained as follows: depending on the applied load, there exists a concentration of stress at the tip of an advancing crack. The stress distribution ahead of the crack tip causes plastic deformation in the region around the crack tip, where the yield stress of the material is exceeded. This plastic deformation causes crack blunting and leads to the relaxation of stresses in the deformed zone. As a result, an impediment in crack growth takes place. The size of the plastic zone ahead of a growing crack increases with decreasing yield strength. The larger the plastic zone, the greater the crack tip blunting and the higher the resistance to crack growth. Thus, matrix softening, which caused a decrease in YS on aging up to 200 hours, led to increased SCC resistance. Increasing Cr depletion of the matrix due to carbide/carbonitride precipitation contributed indirectly to the increased resistance by softening the austenite matrix. Normally, increasing Cr depletion should have led to decreased SCC resistance, because it would lead to the possibility of pre-existing active paths for SCC to occur. However, that was not the case. Decreased resistance because of intergranular SCC (IGSCC) has been reported in dilute chloride solutions for sensitized austenitic alloys.[33,34] But in hot concentrated chloride solutions, these sensitized steels failed by transgranular SCC.[35] The nil effect of the Cr depletion on the SCC resistance was a result of the environment, which, due to its high corrosivity (pH = 4), was not able to differentiate the pre-existing active paths from the strain-generated ones, thus attacking both equally. The small quantity of sigma phase did not have any effect on the SCC resistance of the weld metal aged up to 200 hours.

The decrease in the SCC resistance on aging to 2000 hours was a direct consequence to the significant increase in the value of n, as a result of extensive sigma phase precipitation. This decrease in the SCC resistance could have been due to decreased stress relaxation as a

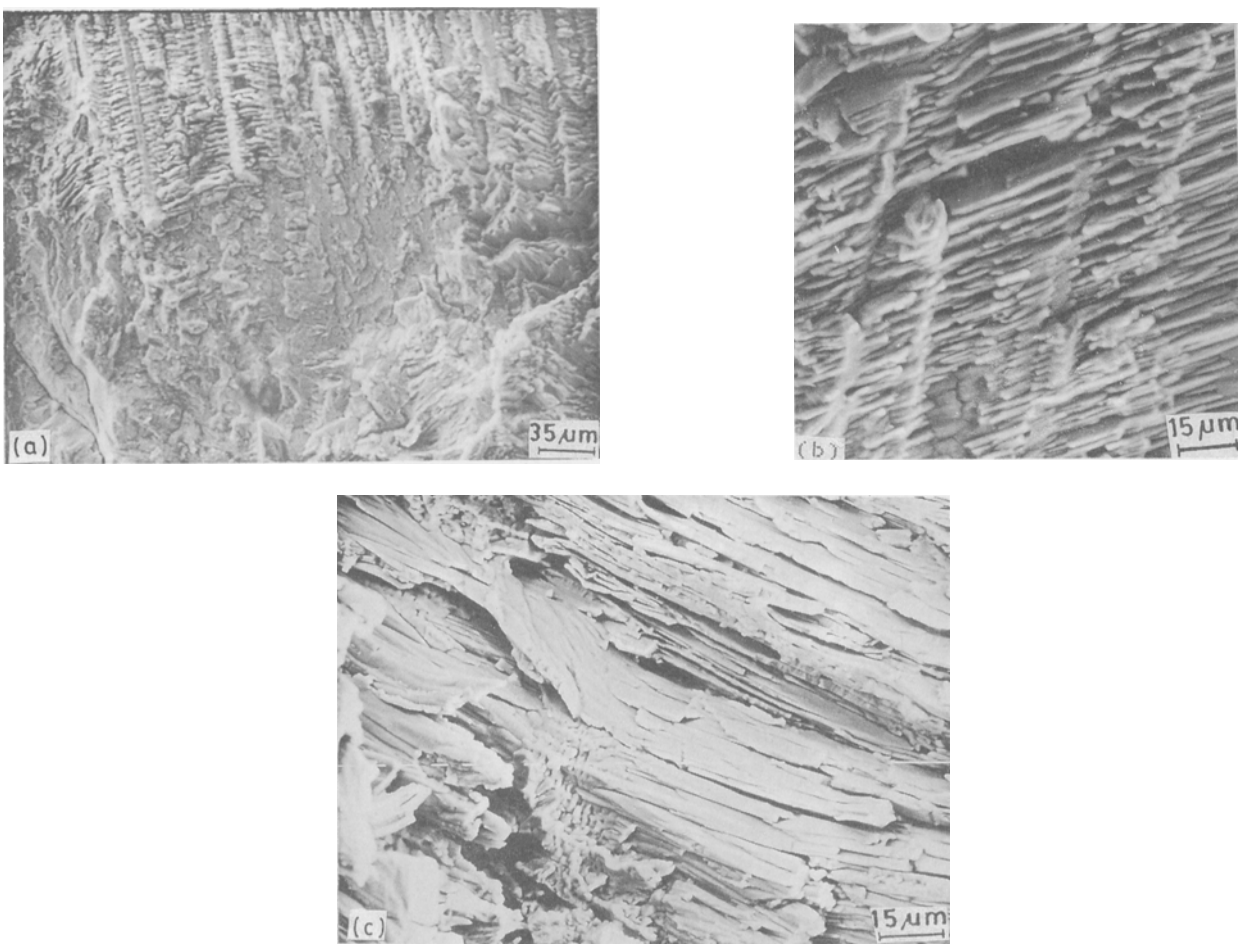

Fig. 14—Typical high-magnification fractographs of weld metal aged at 873 K and tested by CERT in boiling $MgCl_2$ solution at 427 K, showing (*a*) a combination of interface cracking and SCC of austenite, (*b*) interface cracking, and (*c*) SCC of austenite.

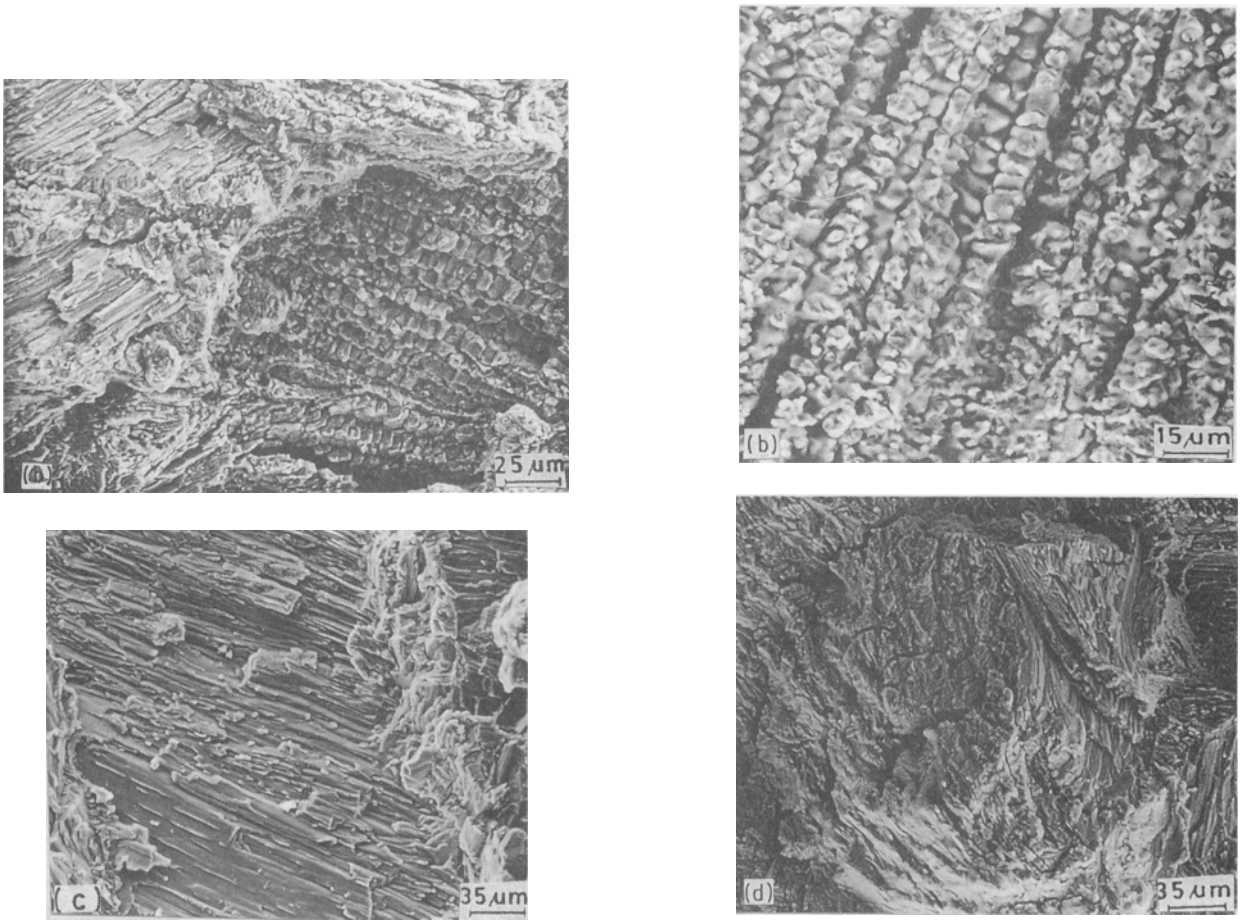

Fig. 15—Typical high-magnification fractographs of weld metal aged at 873 K and tested by constant load technique in boiling $MgCl_2$ solution at 427 K, showing (*a*) a combination of interface cracking and SCC of austenite, (*b*) interface cracking, and (*c*) and (*d*) SCC of austenite.

result of increased particle-dislocation or dislocation-dislocation interaction. Hence, faster crack propagation took place due to reduced blunting of the crack tip. Also, the presence of large amounts of sigma phase would have contributed to faster crack propagation by making available more austenite-sigma interfaces for cracking.

A detailed high-magnification study of the fracture surfaces, as shown in Figures 14(a) through (c) (which pertain to CERT-tested samples) and Figures 15(a) through (d) (which pertain to samples tested by constant load technique), showed that the failure exhibited similar typical features. The failure occurred by a combination (Figures 14(a) and 15(a)) of transgranular SCC (TGSCC) of austenite (Figures 14(c) and 15(c) and (d)) and interphase-interface cracking (Figures 14(b) and 15(b)) in all the heat-treated conditions. This transition to interface cracking was reported by Sherman *et al.*[20] and Stalder and Duquette[21] during SCC of as-deposited weld metal. Sherman *et al.* reported that the crack propagated preferentially along interfaces which were oriented near normal to the tensile stress. Similar, but less severe, interfacial attack was observed by Sherman *et al.* in unstressed specimens. Thus, they attributed the SCC growth to the stress-assisted dissolution of the austenite-ferrite interfaces. Stalder and Duquette attributed this preferential attack of the interface to the nonequilibrium segregation of solute elements in the weld metal. In the present study, the interfaces involved were those of delta ferrite and sigma with austenite.

Available literature suggests that SCC takes place under the influence of two competing factors: (1) slip step formation and (2) dissolution of the slip step produced.[36,37] The transition to IGSCC occurs when the slip step formation rate is greater than the corrosion rate of the slip step. This leads to dislocation pile ups at the grain boundaries, causing stress concentration there, and intergranular dissolution results.[36] Based on similar arguments, when a transgranularly initiated crack in austenite of the weld metal encounters an interface of austenite-ferrite or austenite-sigma, it is arrested since ferrite and sigma are resistant to SCC in chlorides. Further application of load then causes increasing dislocation pileups at the crack tip, leading to a stress concentration at the interface and causing its dissolution. Interface characteristics, such as high dislocation density, vacancies, and impurity atom concentration, would assist the interfacial dissolution.

IV. CONCLUSIONS

1. High-temperature aging of AISI type 316 L weld metal at 873 K led to the precipitation of carbides at shorter aging times and of sigma phase at longer aging times.

2. The two competitive processes of matrix softening and hardening caused changes in the properties of the weld metal. While YS was found to be significantly affected only by matrix softening, matrix hardening considerably influenced UTS and n. Ductility, matrix hardness, and stress-corrosion properties were influenced by both factors. The weld metal aged up to 200 hours showed maximum SCC resistance.
3. The weld metal was found to fail by a combination of TGSCC of austenite and interface cracking in $MgCl_2$, in both the CERT and constant load tests.

ACKNOWLEDGMENTS

The authors wish to thank S. Francis Rajan, V. Chidambaram, A. Varadharaj, S. Thyagarajan, and M. Radhika for their invaluable help during the course of the experiments. They also thank P. Muraleedharan, M.G. Pujar, and A. Veeramani for useful suggestions and discussions.

REFERENCES

1. F.C. Hull: *Weld. J.*, 1967, vol. 46, pp. 399-s-409-s.
2. T.P.S. Gill, M. Vijaylakshmi, P. Rodriguez, and K.A. Padmanabhan: *Metall. Trans. A*, 1989, vol. 20A, pp. 1115-24.
3. R.J. Thomas and D. Yapp: *Weld. J.*, 1978, vol. 57, pp. 361-s-66-s.
4. U.K. Mudali, R.K. Dayal, T.P.S. Gill, and J.B. Gnanamoorthy: *Werkst. Korros.*, 1986, vol. 37, pp. 637-43.
5. T.P.S. Gill, U.K. Mudali, V. Seetharaman, and J.B. Gnanamoorthy: *Corrosion*, 1988, vol. 44, pp. 511-16.
6. A. Garner: *Corrosion*, 1979, vol. 35, pp. 108-14.
7. T.P.S. Gill, J.B. Gnanamoorthy, and K.A. Padmanabhan: *Corrosion*, 1987, vol. 43, pp. 208-13.
8. T.P.S. Gill, M. Vijayalakshmi, J.B. Gnanamoorthy, and K.A. Padmanabhan: *Weld. J.*, 1986, vol. 65, pp. 122-s-28-s.
9. R.G. Thomas and S.R. Keown: *Proc. Int. Conf. on Mechanical Behaviour and Nuclear Application of Stainless Steel at Elevated Temperature*, Varese, Italy, May 20–25, 1981, The Metals Society, London, 1981, pp. 30-38.
10. T.P.S. Gill: Ph.D. Thesis, Indian Institute of Technology, Madras, India, 1984.
11. F.C. Hull: *Weld. J.*, 1973, vol. 52, pp. 104-s-13-s.
12. G.F. Slattery, S.R. Keown, and M.E. Lambert: *Met. Technol.*, 1983, vol. 10, pp. 373-85.
13. H. Kokawa, T. Kuwana, and A. Yamamoto: *Weld. J.*, 1989, vol. 68, pp. 92-s-101-s.
14. V.S. Raghunathan, V. Seetharaman, S. Venkadesan, and P. Rodriguez: *Metall. Trans. A*, 1979, vol. 10A, pp. 1683-89.
15. J.K. Lai and J.R. Haigh: *Weld. J.*, 1979, vol. 58, pp. 1-s-6-s.
16. R.J. Gray, R.T. King, and V.K. Sikka: *J. Met.*, 1978, vol. 30, pp. 18-26.
17. A.L. Ward: *Nucl. Technol.*, 1974, vol. 24, pp. 201-15.
18. W.A. Baeslack III, D.J. Duquette, and W.F. Savage: *Corrosion*, 1979, vol. 35, pp. 45-54.
19. W.A. Baeslack III, W.F. Savage, and D.J. Duquette: *Weld. J.*, 1979, vol. 58, pp. 83-s-90-s.
20. D.H. Sherman, D.J. Duquette, and W.F. Savage: *Corrosion*, 1975, vol. 31, pp. 376-80.
21. F. Stalder and D.J. Duquette: *Corrosion*, 1977, vol. 33, pp. 67-72.
22. H. Shaikh, H.S. Khatak, and J.B. Gnanamoorthy: *Werkst. Korros.*, 1987, vol. 38, pp. 183-87.
23. T.P.S. Gill and J.B. Gnanamoorthy: *Trans. Indian Inst. Met.*, 1983, vol. 36, pp. 269-73.
24. S.R. Keown and R.G. Thomas: *Met. Sci.*, 1981, vol. 15, pp. 386-92.
25. A.A. Tavassoli, A. Bisson, and P. Soulat: *Met. Sci.*, 1984, vol. 18, pp. 345-50.
26. J.M. Leitnaker, G.A. Potter, R.H. Shannon, D.P. Edmonds, R.S. Course, K.F. Russel, and C.W. Houck: Report No. 5400, Oak Ridge National Laboratory, Oak Ridge, TN, 1978.
27. M. Hishida and H. Nakada: *Corrosion*, 1977, vol. 33, pp. 332-38.
28. A. Desestret and R. Oltra: *Corros. Sci.*, 1980, vol. 20, pp. 799-820.
29. M. Hishida, J.A. Begley, R.D. McCright, and R.W. Staehle: *Stress Corrosion Cracking—The Slow Strain Rate Technique*, G.M. Ugiansky and J.H. Payer, eds., ASTM STP 665, 1979, pp. 47-60.
30. C.D. Kim and B.E. Wilde: *Stress Corrosion Cracking—The Slow Strain Rate Technique*, G.M. Ugiansky and J.H. Payer, eds., ASTM STP 665, 1979, pp. 97-112.
31. H.S. Khatak, P. Muraleedharan, J.B. Gnanamoorthy, P. Rodriguez, and K.A. Padmanabhan: *J. Nucl. Mater.*, 1989, vol. 168, pp. 157-61.
32. H.S. Khatak, P. Muraleedharan, J.B. Gnanamoorthy, P. Rodriguez, and K.A. Padmanabhan: *Proc. 6th Int. Conf. on Fracture*, New Delhi, 1984, pp. 153-55.
33. M. Kowaka and T. Kudo: *Trans. Jpn. Inst. Met.*, 1975, vol. 16, pp. 385-96.
34. R.C. Newman, K. Sieradzki, and H.S. Isaacs: *Metall. Trans. A*, 1982, vol. 13A, pp. 2015-26.
35. H.E. Hanninen: *Int. Met. Rev.*, 1979, vol. 24, pp. 85-135.
36. P. Muraleedharan, H.S. Khatak, J.B. Gnanamoorthy, and P. Rodriguez: *Metall. Trans. A*, 1985, vol. 16A, pp. 285-89.
37. M.K. Takano and R.W. Staehle: *Trans. Jpn. Inst. Met.*, 1978, vol. 19, pp. 1-10.